FINITE ELEMENT PREDICTION OF THE EFFECTS OF TOOL RAKE ANGLE ON METAL CUTTING PROCESS

Amor BENMEDDOUR[1]
[1] *Department of Mechanical Engineering, Faculty of Engineering Sciences, University of Brothers Mentouri Constantine1, Road of Ain-el-Bey, 25000 Constantine, Algeria.*
E-mail: omar.meca.2017@Gmail.com

ABSTRACT*: The service life of the parts produced by machining and, in particular as regards its fatigue life are not only related to the surface condition of the part, but also to the residual stress profile induced during machining, which was influenced by the geometrical conditions of the cutting tool. For this reason a coupled thermo-mechanical analysis of a 2D finite element model of the orthogonal metal cutting process is made through the explicit finite element code ABAQUS in order to predict the effects of rake angle of cutting tool on temperature, plastic strain fields, chip morphology and residual stress within a workpiece by using explicit dynamic Arbitrary Lagrangian Eulerian (ALE) technique. The Johnson-Cook model with a damage evolution criterion and its fracture energy are utilized to simulate the chip formation during the cutting process. The simulation results are compared with experimental measurements, which were obtained from the literature. A reasonable agreement was obtained.*

KEYWORDS*: Finite element simulation, Metal Cutting, Damage evolution, Rake Angle, Plastic Strain, Residual Stress.*

1 INTRODUCTION

The Material removal process is one of the most important mechanical parts development processes in the industry. Different types of cutting configurations exist and are applied (orthogonal, oblique and three-dimensional). When machining at high speeds, many parameters are involved and have an influence on the quality of the part to be produced, such as cutting speed, chip thickness, and feed rate, as well as the geometric characteristics of the tool. Many studies and experiments were performed in the early 1940s, and since then, considerable effort has been made in order to develop models capable of correctly predicting the cutting operations. Analytical models of orthogonal metal cutting have been developed by early researchers. for example, Merchant (1945) who proposed an analytical model for the cutting force. Later, this method was used by other researcher (Ren and Altintas, 2000; Karpat and Özel, 2008) to highlight the influence of the geometry of the cutting tool on the cutting parameters during machining. In recent years, FEM based numerical models has been extensively employed for cutting process simulations due to their potential to provide predictions in various process variables such as cutting forces, the stresses, strains and temperatures in the workpiece and in the tool, which can help to optimize cutting processes and tool design, reduce costs and increase productivity. Liu and Guo (2000) studied the influence of tool-chip friction on the residual stresses induced in machined surface layer of AISI 304 steel. Mohammadpour et al. (2010) developed a two-dimensional finite element model of the AISI 1045 steel of the machining process to study the effect of cutting speed and feed rate on the state of induced stresses. A 3D mixed approach model that combine the FEM model and experimental data was used by Rami et al. (2017) to predict the residual stress distribution in the workpiece with a minimum calculation time.

The main advantage of using numerical models is to limit the number of tests, and therefore the cost of an experimental process. The models allow studying the influence of various conditions and geometries of cutting without having to carry out a large number of tests. For this reason and because of the complexity of 3D modeling, a coupled thermo-mechanical analysis of a simplified 2D finite element model was performed in the present study to model orthogonal cutting process of AISI 316L steel based on the Arbitrary Lagrangian

Eulerian (ALE) formulation. The numerical simulations are carried out using the finite element software package ABAQUS/Explicit. The Johnson-Cook equation with damage evolution is used to describe the workpiece material behavior and chip formation. The influence of the rake angle on the temperature and stress distributions, chip morphology and residual stress profile in the orthogonal machining process are revealed.

2 FINITE ELEMENT MODELING

In this paper, as part of cutting modeling, we chose to adopt the Lagrangian-Eulerian Arbitrary formulation (A.L.E.), often used by researchers (Movahhedy et al., 2000; Gadala et al., 2002), and rather adapted to the 2D stationary cutting modeling. In addition, this approach minimizes the distortion of the mesh often encountered during the simulation. Figure 1 shows the geometry and boundary condition of the proposed numerical model. The plane strain condition is assumed for the deformations in the orthogonal cutting process simulation which was developed with Abaqus/Explicit software. The workpiece and a cutting tool are meshed with, respectively, 11256 and 702 isoparametric four-node plan strain thermo-mechanical coupled quadrilateral continuum elements, with reduced integration and automatic hourglass control (CPE4RT). In order to accurately predict the strain and stress fields and chip morphology, a finer mesh are used in the area where the machining will take place in the workpiece and round the tool edge in which high stress gradients occur.

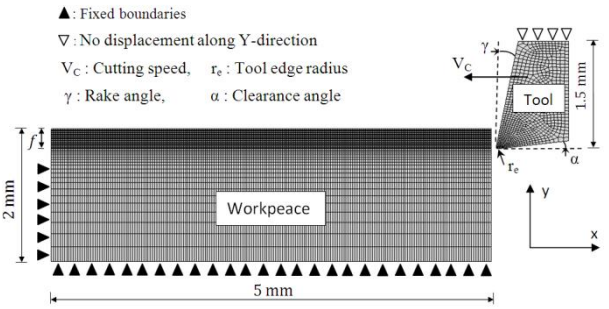

Figure 1. 2D FEM geometry model and boundary condition

The workpiece material was fixed in x and a y direction, the cutting speed of 400 m/min is applied to the tool in the x direction. The depth of cut has been set to 0.2 mm, the rake angle change from -9° to 15°, the clearance angle is 7°, the cutting tool edge radius is 20 μm and the initial temperature was assumed to be 20 °C. The physical properties of the workpiece (AISI 316L) and the cutting tool materials (Kennametal K313) were obtained from Johnson and Cook (1983) and they are summarized in Table 1.

Table 1. Properties of workpiece material and tool material (Johnson and cook, 1983).

Properties	Workpiece materials (AISI316L Steel)	Cutting tool materials (Kennametal K313)
Density (ρ, Kg/m^3)	8000	14900
Young's Modulus (E, GPa)	193	615
Poisson Ratio (ν)	0.3	0.22
Specific Heat (Cp, J/Kg°C)	500	138
Thermal Conductivity (k, W/m°C)	20	79
Melting temperature (°C)	1400	—
Thermal expansion coefficient (α, °C^{-1})	19.9 x 10^{-6}	—

2.1 Johnson-Cook Constitutive Model

The Johnson and Cook (1983) plasticity model is widely used to describe the material behavior at large strains and high strain rates. The model is expressed by the equivalent plastic flow stress as shown in Eq. (1).

$$\sigma_e = \left[A + B\left(\varepsilon_e^P\right)^n\right]\left[1 + C\ln\left(\frac{\dot{\varepsilon}_e^p}{\dot{\varepsilon}_0}\right)\right]\left[1 - \left(\frac{T - T_r}{T_m - T_r}\right)^m\right]$$

where σ_e is the equivalent plastic flow stress, ε_e^P and $\dot{\varepsilon}_e^p$ are respectively the equivalent plastic strain and the equivalent plastic strain rate, $\dot{\varepsilon}_0$ is the reference strain rate ($1s^{-1}$), T_m and T_r are the melting and the room temperature, respectively. *A* is the yield stress, *B* is the strain hardening coefficient, n is the strain hardening exponent, *C* is the strain rate sensitivity factor, m is thermal softening. The Johnson Cook parameters which are adopted from Chandrasekaran et al. (2005) are presented in Table 2.

Table 2. Johnson cook parameters for AISI 316L steel (Chandrasekaran et al., 2005)

A [MPa]	*B* [MPa]	*C*	*n*	*m*
305	1161	0.01	0.61	0.517

2.2 Chip Failure Criteria

The chip formation process is assumed to undergo two steps prior to complete ductile failure.

The first stage considers the initiation of the damage, while the second considers the evolution of the damages.

Damage initiation: The Johnson–Cook fracture model was used as a damage initiation criterion to model material fracture. The Johnson–Cook failure model is based on the accumulated damage. Fracture is assumed to occur when the damage parameter, D, reaches or exceeds the value of one. D is defined as:

$$D = \sum \frac{\Delta \varepsilon_P}{\varepsilon_{pf}}$$

where $\Delta\varepsilon_P$ is the increment of equivalent plastic strain, ε_{Pf} is the equivalent fracture strain, which is given by:

$$\varepsilon_e^p = \left[D_1 + D_2 \exp\left(D_3 \frac{\sigma_m}{\sigma_e}\right)\right]\left[1 + D_4 \ln\left(\frac{\dot{\varepsilon}_e^p}{\dot{\varepsilon}_0}\right)\right]\left[1 + D_5\left(\frac{T - T_r}{T_m - T_r}\right)\right]$$

where $D_1 - D_5$, are the damages parameters and are determined by experiment. σ_m is the hydrostatic pressure and σ_e is the von-Mises stress. The adopted J–C damage constants of AISI 316L steel were selected from Ruin et al. (2017) and are given in Table 3.

Table 3. The J–c damage constants of AISI 316l (Ruin et al., 2017)

D_1	D_2	D_3	D_4	D_5
0.05	3.44	2.12	0.002	0

Damage evolution: For the description of the failure evolution, the second step consists in using a damage model evolution based on the fracture energy approach, proposed by Hillerborg's et al. (1976). The law of evolution of the damage is specified in terms of dissipation energy at the fracture G_f. This energy is calculated between the moment of appearance of the damage (characterized by a deformation ε_{oi}) and the instant at the total failure of the element (characterized by a deformation ε_{of}), that is to say between the point's "*c"* and "*d"* in Figure.2:

$$G_f = \int_{\varepsilon_{oi}}^{\varepsilon_f} L\,\sigma_0\,d\varepsilon = \int_0^{u_f} \sigma_0\,du$$

This expression of Gf introduces the definition of equivalent plastic displacement (u) after the occurrence of the damage and the work per unit area of the crack. The implementation of this stress-strain concept in a finite element model requires the definition of a characteristic length (L) which depends on the geometry and the size of the mesh. It is calculated at the integration point and is a function of the element area. This definition is adopted because the direction of propagation of the crack is unknown at this level. This law of damage evolution describes the rate of degradation of the stiffness of the material. It can be linear or exponential. The linear form is written:

$$D = \frac{L_\varepsilon}{u_f} = \frac{u}{u_f}$$

where equivalent the plastic displacement to the fracture is calculated from G_f:

$$u_f = \frac{2G_f}{\sigma_0}$$

The exponential form, used in the chip, has for equation:

$$D = 1 - \exp\left(-\int_0^u \frac{\sigma}{G_f}\,du\right)$$

In order to implement damage evolution criterion and simulate the chip separation, the value of fracture toughness K_C is required to calculate the fracture energy G_f for mode I based on the following equation.

$$G_f = \left(\frac{1 - \nu^2}{E}\right) K_{IC}^2$$

For AISI 316L the fracture toughness of material value for mode I damage evolution used as input data in Abaqus/explicit is 51.3 Mpa$\sqrt{m}$ taken from Čolić et al. (2017).

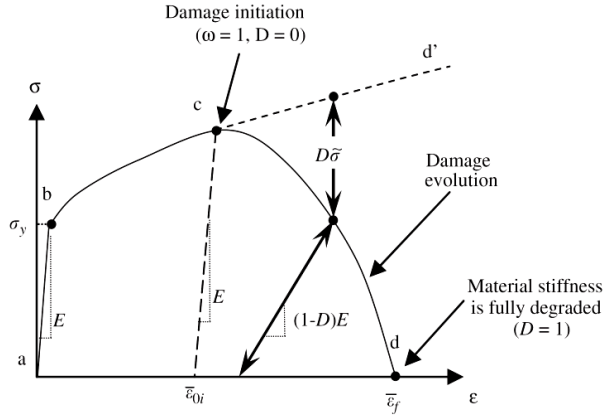

Figure 2. Stress-stain curve with progressive damage degradation (H. K. S., 2011)

2.3 Frictional Model

The most realistic description of frictional normal and shear stress at chip/tool interface has

been proposed by Zorev et al. (1963) friction model As illustrated in Figure 3, two zones exist in the contact zones between the chip and the tool rake face, named the sliding region and the sticking region. The sliding zone obeys the Coulomb friction model while in the second so-called "sticking zone" near the tip of the tool where the frictional stress (τ_f) is assumed to be equal to the shear strength of the machined material (τ_{crit}). The whole contact zone of the chip and the tool rake face can be described by the modified Coulomb friction model which has been used in many previous publications in metal cutting simulations (Zemzemi et al., 2009; Strenkowski and Moon, 1990) as follow:

$$\tau_f = \mu\sigma_n \quad \text{when} \quad \mu\sigma_n < \tau_{crit} \quad \text{(sliding zone)}$$
$$\tau_f = \tau_{crit} \quad \text{when} \quad \mu\sigma_n \geq \tau_{crit} \text{ (sticking zone)}$$

where τ_f is frictional shear stress, σ_n is frictional normal stress, τ_{crit} is the shear stress limit of the workpiece material, and μ is the friction coefficient at the tool-chip contact along the sliding zone and is assumed to be 0.2.

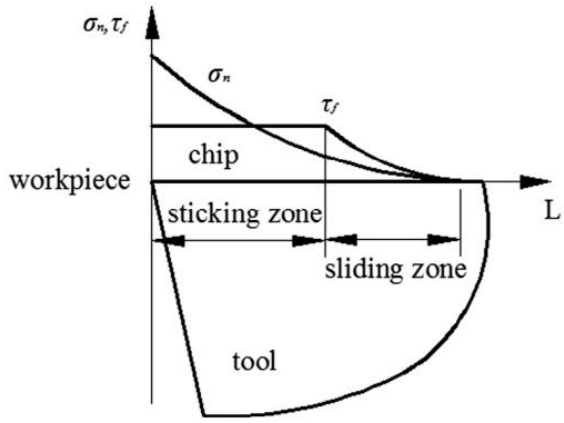

Figure 3. Normal and frictional stress distributions at chip-tool interface

2.4 Heat transfer modelling

During the cutting process, a significant heating is generated. The heat in the workpiece and the cutting tool comes mainly from the heat generated by friction at the tool-chip interface and by the plastic working of the workpiece material generated during machining. The transfer of this heat into both the chip and the workpiece and between the chip and the tool is assumed to be performed by conduction. To simplify the study we neglected radiation. The heat transfer by conduction is defined by the following equation:

$$k\left[\frac{\partial^2 T}{\partial x^2}+\frac{\partial^2 T}{\partial y^2}\right]-\rho c\left[u\frac{\partial T}{\partial x}+v\frac{\partial T}{\partial y}\right]+\dot{Q}_g=0$$

where k is the thermal conductivity, ρ is the density, *c* is the specific heat, and Qg is the volumetric heat generation rate. The volumetric heat flux generated from plastic work can be found from :

$$\dot{q}_p = \eta_p \bar{\sigma}\dot{\varepsilon}_p$$

where n_p is the fraction of the friction energy converted to heat and is assumed to be equal to 0.9 in the current work. σ is the effective stress. The heat flux density generated by friction at the tool / chip interface is given by the following relation:

$$\dot{q}_f = \eta_f \tau_f V_s \quad \text{and} \quad q_{Tool} = f_f \dot{q}_f$$

where η_f is the fraction of the energy generated by friction work and converted into heat, τ_f is the friction stress, *Vs*, and f_f are respectively, the sliding velocity, and fraction of the heat transmitted to the cutting tool. q_{Tool} is the heat flow created by the friction of the material at the interface and transmitted to the tool.

3 NUMERICAL RESULTS AND DISCUSSION

Numerical modeling of chip formation has been developed and a series of simulations has been realized to highlight and know the influence of the rake angle of the tool on certain quantities which are inaccessible by experience.

3.1 Model Validation

In the first part of this study, in order to verify the accuracy of the proposed model and simulation of orthogonal cutting of AISI 316L steel, the residual stress field obtained numerically was compared with the experimental results obtained by M'Saoubi et al. (1999) under similar cutting conditions. the conditions adopted in the case of this modeling for validation were: rake angle is 0°, clearance angle = 7°, cutting edge radius *R* = 0.02 mm, cutting speed *V* = 100 m/min, friction coefficient = 0.2, feed rate *f* = 0.1 mm. Figure 4(a, b) shows the experimental and predicted axial residual stress (σ_{11}) and circumferential residual stress (σ_{33}) profiles on the workpiece.

The observation of Figure 4 shows that the profiles of residual stress curves predicted by simulation have the same appearance compare with those measured by experience, these curves are characterized by a state of tensile stresses on the surface of the machined part and with as the depth of the workpiece increases, the tensile stresses decrease rapidly and reach a state of compression

stresses, and as the depth of the workpiece increases, the amplitude of the compressive residual stress decrease gradually to become zero.

In Figure 4 (a), The maximum axial tensile stress σ11 predicted by simulation occurs on the surface of the machined part is reached the value of 798.6 MPa. The compressive stress reaches the maximum value of 102 MPa at a depth of 0.2 mm. Comparing these results with those measured by experience, the values of the maximum tensile stress reached at the surface are very close. With regard to the residual compressive stresses, the difference between the maximum numerical and experimental values does not exceed 20 MPa.

In Figure 4 (b), the maximum circumferential tensile stress σ_{33} appears on the surface of the machined workpiece and has a maximum value of 581.8 MPpa which is very close to that measured. However, it can be noted that, there are large deviation (37.2%) between the maximum predicted circumferential compressive stress σ_{33} the experimental one. The finite element model approach accurately predicted the residual stress contour shape and trends. Furthermore, the predicted maximum value of tensile axial residual stress σ11 and its depth into the workpiece was very close to the experimental one. Therefore, it is important to note that the proposed EF model with the selected parameters such as the choice of the mesh, the JC equation model with a damage evolution criterion parameters and the friction coefficient value indicates the satisfactory capability of the proposed model to predict the residual stress induced by machining and can be use to simulate the orthogonal cutting of AISI 316L.

3.2 The Effect of Rake Angle on Chip Formation

In this section, we analyze the effect different rake angle on chip type produced during cutting machining. The morphology of the chip depends on the thermal and mechanical characteristics of the material to be machined and its response to the thermo mechanical loadings it undergoes during machining, as well as the friction at the interface tool/chip (Zemzemi et al., 2009).

Simulations were performed with four different rake angles of -9°, 0°, 9° and 15°. In this case the cutting speed is considered to be constant as 400 m/min, cutting depth 0.2 mm and the clearance angle are set as 7°. Figure 5 illustrates the temperature distribution of the workpiece, chip and tool, as well as the chip morphology for various tool angles of material removal. We can clearly observe that, the rake angle has a great influence on the chip shape created by machining, the chip shape changes from discontinuous chip to continuous chip with increasing the tool rake angle. When the cutting angles are negative, in our case we have taken the tool rake angle of -9 °, the formation of chips is broken and we notice the formation of a number of unconnected segments and increasing the rake angle of the tool up to the value of 15°, the number of these segments gradually decreases until a fully connected chip and consequently continuous chip is formed. It should be noted that by increasing the rake angle from negative to positive values, the length of the interface has been reduced, of course in the hypothesis of a 2D model, since in reality it is the contact surface that will decrease, and consequently the compression on the chip decreases, resulting in decreasing the values of

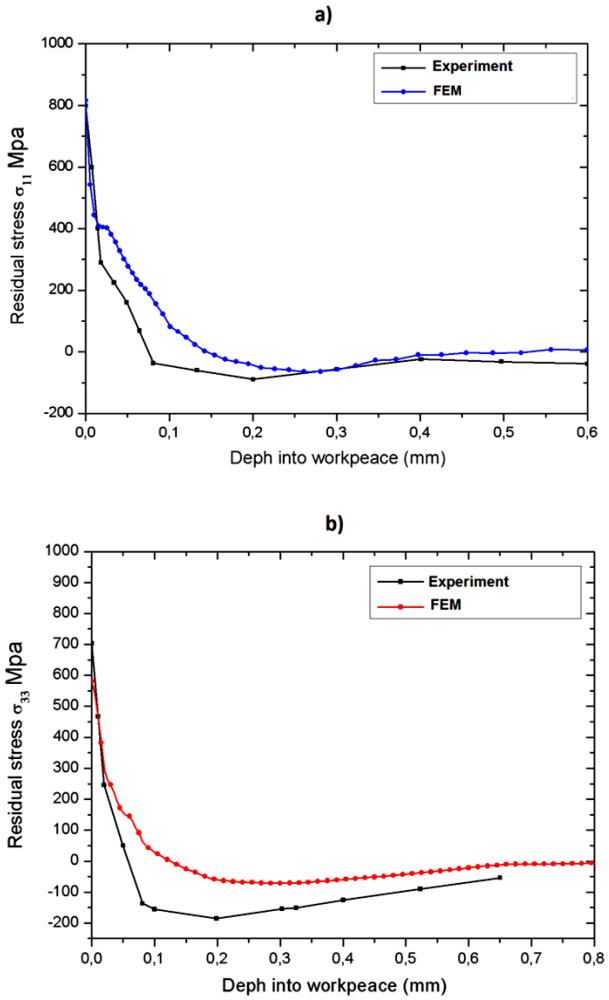

Figure 4. Comparison of residual stress profiles between simulation and experiment: a) in cutting direction (σ_{11}), b) in the circumferential direction (σ_{33}).

shear stress in the primary shear zone, and consequently therefore favors the formation of

continuous chips. However, it is important to note that a large increase in the rake angle could result in an insufficient tool rake angle to withstand the stress generated during cutting process (Olovsson et al., 1999). The shape of chip play an important role in the process stability. In general, the continuous chip and, because of the damages created in the periphery of the cutting tool, which could affect the proper functioning of the machine is undesirable in industrial applications.

3.3 Effect of rake angle on temperature

Fig. 5 shows the temperature distribution of the workpiece material during steady-state cutting process for various different rake angles. It can be seen that the effect of the tool rake angle on temperature distribution is significant, when increasing tool rake angle from -9° to 15°, the maximum temperature reduces rather remarkably from 830 °C to 565 °C. The high temperature along the tool-chip interface are observed in the secondary deformation zone at negative tool rake angle, this is attributed to local heating caused by friction between the tool and the chip and increase contact length and pressure at the chip interface at negative rake angle.

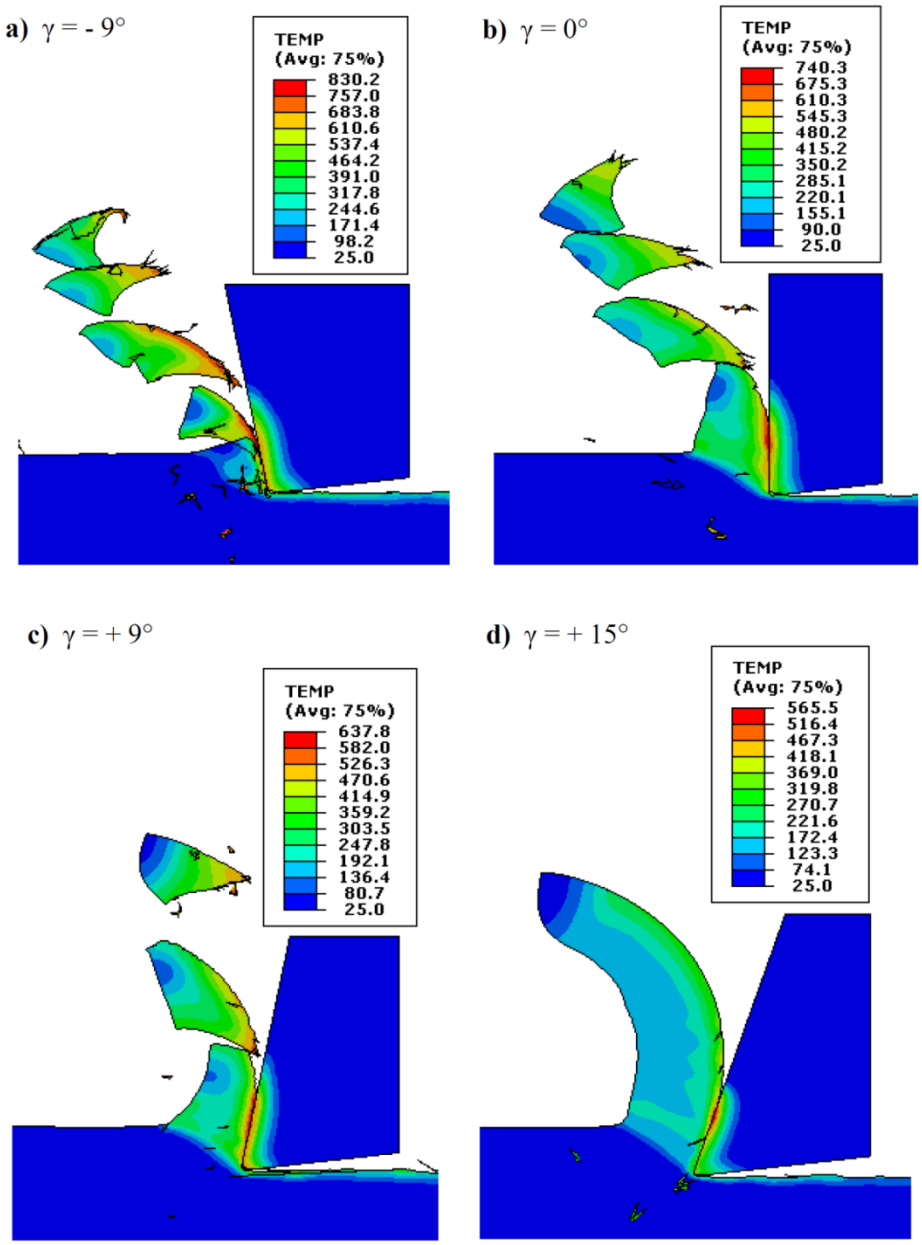

Figure 5. The temperature distribution (C°) and Chip formation at different rake angles in cutting speed of 400 m/min and feed rate of 0.2 mm/rev, a) γ = -9° , b) γ = 0°, c) γ = +9°, d) γ = +15°.

3.4 Effect of rake angle on plastic strain

Figure 6 shows the distribution of the equivalent plastic strain (PEEQ) in the workpiece, chip and tool at different rake angles. The results show very high plastic strain in the chip at the secondary deformation zone (SDZ) at the chip-tool interface; this is due to the severe deformation of the material caused by highly pressure exerted by the tool on the chip surface. It is clearly observed, that increasing the tool rake angle induces a decreasing plastic strain level, when the rake angle change from -9° to 15°, the high values of plastic strain at the chip-tool interface increase from 3.63 to 2.29.

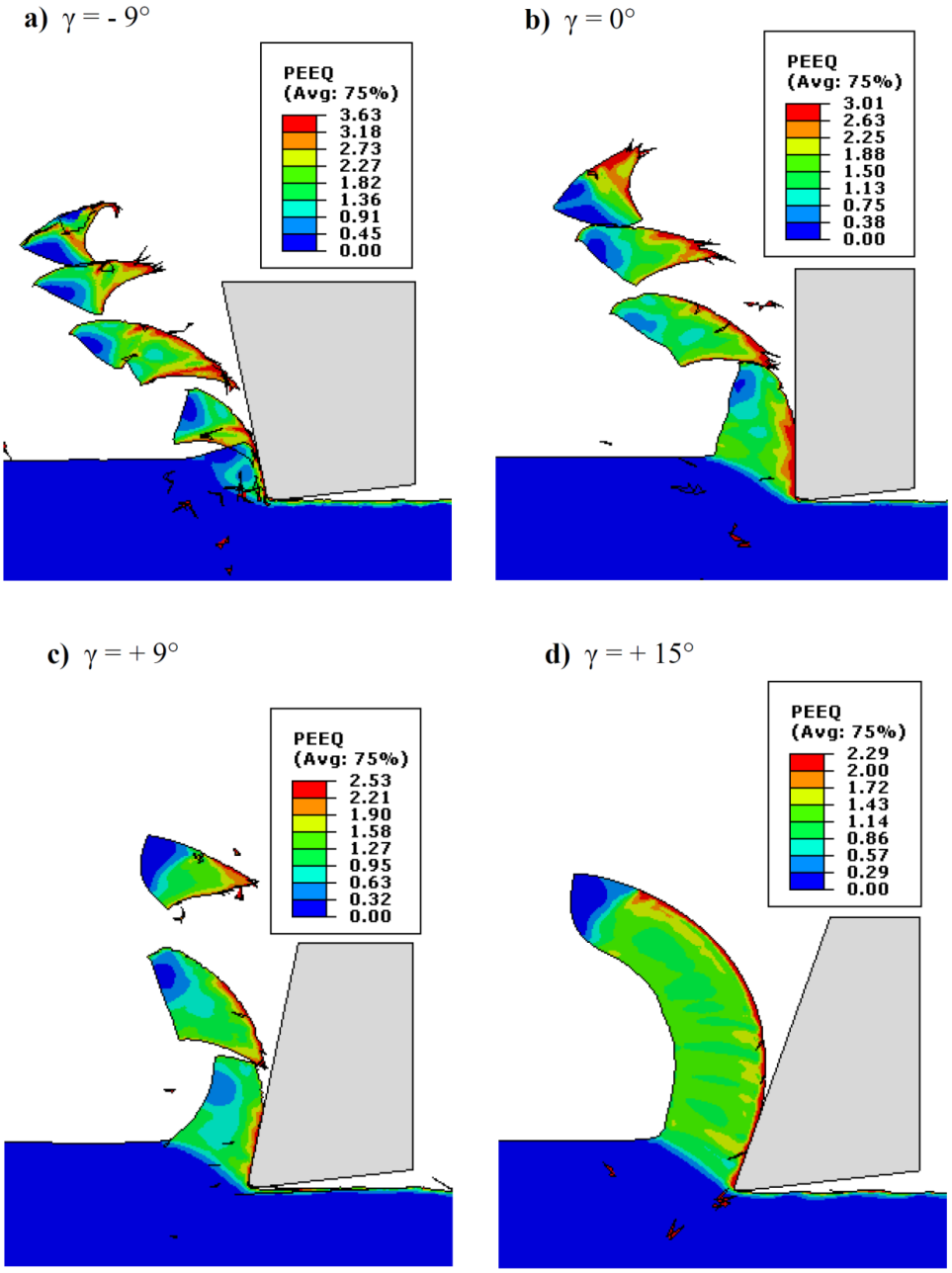

Figure 6. Strain distribution and Chip formation at different rake angles in cutting speed of 400 m/min and feed rate of 0.2 mm/rev, a) γ = -9° , b) γ = 0°, c) γ = +9°, d) γ = +15°.

3.5 Effect of rake angle on residual stress

In order to study the influence of the rake angle on residual stresses induced in the workpiece material. Simulations were performed with four different rake angles of -9°, 0°, 9° and 15°. The axial stresses (σ_{11}) evolution in the cutting direction versus the workpiece depth at different tool rake angles are plotted in Figure 7. We can observe that level of the tensile stress is lowered when the inclination angle of the tool is decreased from negative to positive value and the level of compressive stress layer is also increased when the inclination angle of the tool is decreased. The

maximum value axial tensile stress was decreased from 1170.7 MPa to 543.8 MPa and the maximum compressive stress, increase from 24.9 Mpa to 110.4 Mpa when the rake angles were increased from -9° to 15°. The results of the effect of the rake angle on residual stresses induced after machining operations are of great interest to the industry. It is generally observed that positive rake angles generate machined surfaces of the workpiece with higher quality than the negative rake angle, and it is found that a tool with positive rake angle requires about low force and power less than a tool with negative rake angle, therefore in the industry the tool with positive angle are usually selected for finishing machining operations. Qualitatively, this important result is in complete agreement with Miguélez et al. (2009).

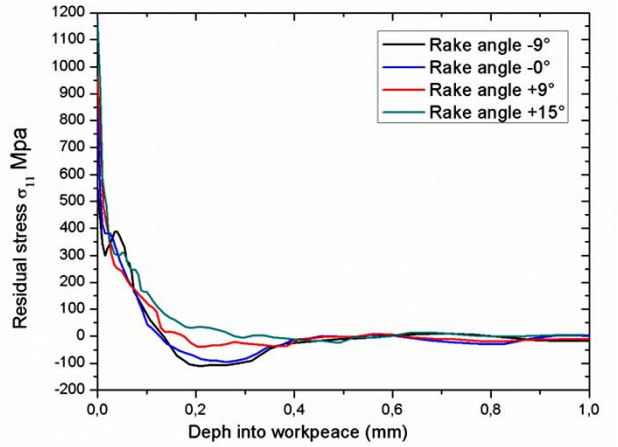

Figure 7. Effect of the tool rake angle on the axial residual stresses (σ_{11}).

4 CONCLUSION

A two-dimensional finite element model has developed to simulate the orthogonal cutting process of AISI 316 L steel. The effects of tool rake angle on temperature fields residual stresses and plastic strain as well as chip formation has been carried out. The main findings from this investigation are summarized below.

1) The model was validated through the comparison with experimental and numerical results reported in the literature, the ability of the model to predict both residual stress and chip morphology is also proven for various cutting angles. The predicted temperature and residual stress fields induced by machining can help better understanding the cutting tool wear during the turning process. This approach represents a substantial reduction in costs and time compared with experiments.

2) The effect of the tool rake angle on temperature, stress and strain distribution in the worckpeace is significant, increasing the rake angle from -9° to 15° decreasing the temperature and the plastic strain in the workpiece.

2) The rake angle has a strong effect on the chip morphology, the chip shape changes from discontinuous chip to continuous chip with increasing the tool rake angle from negative to positive values.

4) The numerical prediction of the residual stress distributions on the machined surface was successfully achieved. This study showed that it is possible to reduce the axial residual stresses by increasing the rake angle of the tool. On the other hand, the axial compressive stress will increase.

5 REFERENCES

Merchant, M. E. (1945). *Mechanics of the Metal Cutting Process*, Journal of Applied Physics, Vol. 16, No. 5, pp. 267–275.

Ren, H., Altintas, Y. (2000). *Mechanics of machining with chamfered tools*, Transactions of the ASME, Journal of Manufacturing Science and Engineering, Vol. 122, No. 4, PP. 650–659.

Karpat, Y., Özel, T. (2008). Analytical and thermal modeling of high-speed machining with chamfered tools,Journalof Manufacturing Science and Engineering, Vol. 130, No. 1, pp. 1–15.

Liu, CR., Guo, YB. (2000). *Finite element analysis of the effect of sequential cuts and too-chip friction on residual stresses in a machined layer*, International Journal of Mechanical Sciences, Vol. 42, No. 6, pp. 1069–1086.

Mohammadpour, M., Razfar, MR., Jalili Saffar, R. (2010). *Numerical investigating the effect of machining parameters on residual stresses in orthogonal cutting*, Simulation Modelling Practice and Theory, Vol.18, No. 3, pp. 378–389.

Rami, A., Kallel, A., Sghaier, S., Youssef, S., Hamdi, H. (2017). *Residual stresses computation induced by turning of AISI 4140 steel using 3D simulation based on a mixed approach*, *International Journal of Advanced*

Manufacturing Technology, Vol. 91, No. 9, pp. 3833–3850.

Movahhedy, M., Gadala, M.S., Altintas, Y. (2000). *Simulation of the orthogonal metal cutting process using an arbitrary Lagrangian Eulerian finite-element method*, Journal Of Materials Processing Technology , Vol. 103, No. 2, pp. 267–275.

Gadala, M.S., Movahhedy, M.R., Wang, J. (2002). *On the mesh motion for ALE modeling of metal forming processes*, Finite Elements in Analysis and Design, 38,No. 5, pp. 435–459.

Johnson, G. R., Cook, W. H. (1983). *A Constitutive Model and Data for Metals*, Proceedings of the Seventh International Symposium on Ballistics, The Hague, The Netherlands, April 19–21, Vol. 21, pp. 541–547.

Chandrasekaran, H., M'Saoubi, R., Chazal, H. (2005). *Modelling of material flow stress in chip formation process from orthogonal milling and split Hopkinson bar tests*, Materials Science and Technology, Vol. 9, No. 1, pp. 131–145.

Johnson, G.R., Cook, W.H. (1985). *Fracture characteristics of three metals subjected to various strains, strain rates, temperatures and pressures*, Engineering Fracture Mechanics, Vol. 21,No. 1, pp. 31–48.

Ruin Aheli, M., Mirzai, M. A., Hemmati, S. J. (2017). *The Experimental and Numerical Study of Hexagonal Cutting of AISI 316L Steel Round Bars*, IJMF, Iranian Journal of Materials Forming, Vol. 4, No. 2, pp. 37-50.

Hillerborg, A., Modeer, M., and Petersson. P. E. (1976). *Analysis of Crack Formation and Crack Growth in Concrete by Means of Fracture Mechanics and Finite Elements*, Cem. Concr. Res., Vol 6, No 6, pp. 773-781.

H. K. S. 2011, "ABAQUs/Explicit Analysis User Manual," Version 6.11.

K. Čolić, N. Gubeljak, M. Burzić, A. Sedmak, T. Mijatović, A. Milovanović. (2017). *Analysis of fracture behaviour of thin s316l stainless steel plates*, Structural integrity and life, Vol. 17, No 3, pp. 211–216.

Zorev, NN. (1963). *Interrelationship between shear processes occurring along tool face and shear plane in metal cutting*, Proceedings of the Conference on International International research in production engineering, ASME, New York, pp. 42–49.

Zemzemi, F., Rech, J., Ben Salem, W., Dogui, A., Kapsa, P. (2009). *Identification of a friction model at tool/chip/workpiece interfaces in dry machining of AISI4142 treated steels*, Journal of Materials Processing Technology, Vol. 209, No. 8, pp. 3978–3990.

Strenkowski, J.S., Moon, K.J. (1990). *Finite element prediction of chip geometry and tool/workpiece temperature distributions in orthogonal metal cutting*, ASME Journal of Engineering for Industry, Vol. 112, No. 4, pp. 313–318.

M'Saoubi, R., Outeiro, J. C., Changeux, B., Lebrun, J. L., Morao Dias, A. (1999). *Residual Stress Analysis in Orthogonal Machining of Standard and Resulfurized AISI 316L Steels*, Journal of Materials Processing Technology, Vol. 96, No. 1, pp. 225–233.

Olovsson, L., Nilsson, L., Simonsson, K. (1999). *An ALE formulation for the solution of two-dimensional metal cutting problems*, *Computers and Structs*, Vol. 72, No. 4, pp. 497–507.

Miguélez, M.H., Zaera, R., Molinari, A., Cheriguene, R., Rusinek, A. (2009). *Residual stresses inorthogonal cutting of metals: the effect of thermo mechanical coupling parameters and of friction*, Journal of Thermal Stresses, Vol. 32, No. 3, pp. 269–289.